ELSEVIER

Journal of Chromatography A, 827 (1998) 175–191

JOURNAL OF CHROMATOGRAPHY A

Design of the simulated moving bed process based on adsorption isotherm measurements using a perturbation method

Christian Heuer[a,*], Ernst Küsters[b], Thomas Plattner[b], Andreas Seidel-Morgenstern[c]

[a]*AnalytiCon AG, Separation Technologies, Hermannswerder Haus 17, D-14473 Potsdam, Germany*

[b]*Novartis Pharma AG, Chemical and Analytical Development, S-145.6.54, CH-4002 Basel, Switzerland*

[c]*Otto-von-Guericke-Universität Magdeburg, Max-Planck-Institut für Dynamik komplexer technischer Systeme, D-30106 Magdeburg, Germany*

Abstract

The design of a simulated moving bed (SMB) chromatography process for the enantioseparation of 1-phenoxy-2-propanol with Chiralcel OD as stationary phase is described using equilibrium theory and a dispersion model. The most essential prerequisite for reliable process simulation is the proper experimental determination of the corresponding adsorption isotherms. This paper evolved from the need to: (i) elaborate a technique for adsorption isotherm measurement based on a perturbation method; and (ii) to demonstrate the applicability of the equilibrium-dispersion model for quick process design. The accuracy of the obtained adsorption isotherms was evaluated by comparison with results that have been obtained independently using the classical adsorption–desorption procedure. As the main result, it turned out that the suggested SMB design concept based both on adsorption isotherms measured with the perturbation method and on the equilibrium-dispersion model could be verified experimentally.

Keywords: Adsorption isotherms; Simulated moving bed chromatography; Enantiomer separation; Phenoxypropanol

1. Introduction

Simulated moving bed (SMB) chromatography has emerged as a promising technology allowing the continuous counter-current separation of a feed mixture into two streams of products. It has the potential to offer increased productivity and reduced mobile phase consumption in comparison to batch elution chromatography, which is still the prevailing technique in preparative chromatography. The SMB process, developed in the early 1960s [1], has been used for many years in the petrochemical and sugar industries for large scale separations. In these instances the chromatographic systems are characterised by high saturation capacities of the stationary phases applied and linear adsorption isotherms of the components to be separated. For this, appropriate operating conditions for the SMB separator are easy to access [2]. Recently, the growing demand for efficient methods to purify optical isomers promotes the application of the SMB principle in a smaller scale for more difficult enantioseparations in the pharmaceutical industry [3–13]. However, chiral stationary phases usually exhibit low values of the saturation capacity connected with non-linear adsorption isotherms and strong competition of the components for the available adsorption sites. This results in a more complex SMB design and optimisation compared to the situations mentioned above. The successful development of new applications in the pharmaceutical industry requires a reliable theoretical concept to predict the behaviour of the SMB

*Corresponding author.

0021-9673/98/$ – see front matter
PII: S0021-9673(98)00797-3

separator in order to specify optimal operating conditions for the separation problem considered.

In the present work quantitative predictions are attempted for designing the SMB process. Experimental results for the separation of a racemate will be compared with calculations based on an equilibrium-dispersion model to describe the concentrations in the columns. The model equations can be solved numerically using an algorithm proposed recently by Kniep and Seidel-Morgenstern [14,15]. The applied model requires as the main information the adsorption isotherms. These cannot be predicted and have to be determined in preliminary experiments. For this, a perturbation method based on experiments with racemic mixtures will be used. To evaluate the influence of the applied isotherm determination method on the accuracy of the predictions of the SMB process, an additional comparison based on isotherms measured with the classical adsorption–desorption method will be also presented.

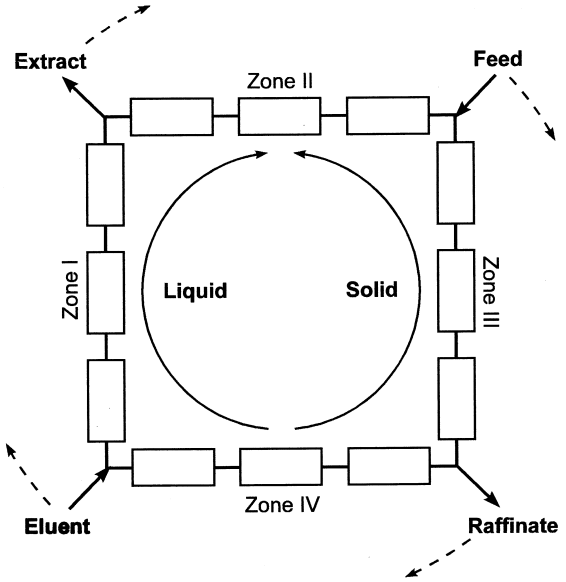

Fig. 1. Schematic representation of a four-zone SMB separator studied.

2. Principle of SMB chromatography

The principle of the SMB separator is represented schematically in Fig. 1. The adsorbent is fixed in columns connected in series. Two incoming and two outgoing liquid streams divide the unit into four sections or zones. Each of the four zones (I, . . . , IV) consists of at least one column and has to fulfil distinct tasks [16]. At the feed point and at the eluent point the feed mixture to be processed and the fresh desorbent (or eluent) are introduced into the unit, respectively. At the points of withdrawal the extract stream enriched with the more retained component and the raffinate stream enriched with the less retained component leave the unit. The desorbent flowing out of zone IV is recycled to zone I. The flow of adsorbent is simulated by shifting the in- and outlet positions at a constant time interval in the direction of the liquid flow. The shifting of the incoming- and outgoing ports mimics an apparent solid flow opposite to the direction of the liquid flow. The shifting period is linked to the solid flow-rate of an equivalent true moving bed. In order to achieve separation of the feed components the internal flow-rates of the liquid phase within the four zones and the shifting period corresponding to the apparent flow of the solid phase have to be specified. To find these operating conditions is a crucial problem in designing the SMB process.

3. Theory

3.1. Mathematical model

The model used in this work to simulate the SMB process and the numerical method developed to solve the mass balance equations have been discussed in detail elsewhere [14,15,17]. Here we give only a brief description.

The equilibrium-dispersion model [17] can be applied to predict the concentration profiles in all columns. Assuming that: (i) there is a permanent equilibrium between the liquid and the solid phases; and (ii) the contributions to band broadening caused by axial dispersion and mass transfer resistances can be described by an apparent dispersion coefficient, D_{ap}, as a lumped parameter, the following mass balance equation of a component i has to be solved for each column j of the SMB unit:

$$\frac{\partial C_i^j}{\partial t} + \left(\frac{1-\varepsilon}{\varepsilon}\right)\frac{\partial q_i^j}{\partial t} + u_j \frac{\partial C_i^j}{\partial z^j} = D_{\mathrm{ap}_i}\frac{\partial^2 C_i^j}{\partial z^{j^2}},$$
$$i = 1, \ldots, N_{\mathrm{Comp}}, \quad j = 1, \ldots, N_{\mathrm{Col}} \tag{1}$$

In this equation ε is the total porosity of the columns and u_j is the linear velocity of the liquid phase in column j. The concentrations of component i in the liquid and in the solid phases, C_i and q_i, respectively, are related through the adsorption isotherms:

$$q_i = f(C_1, C_2, \ldots, C_N), \quad i = 1, \ldots, N_{\mathrm{Comp}} \tag{2}$$

The apparent dispersion coefficient for a column of length L can be estimated from the number of theoretical plates N_P according to:

$$D_{\mathrm{ap}_i} = \frac{uL}{2N_{P_i}(u)}, \quad i = 1, \ldots, N_{\mathrm{Comp}} \tag{3}$$

The solution of Eq. (1) requires suitable initial and boundary conditions. Assuming not preloaded columns at the beginning of the process holds:

$$C_i^j(z, t=0) = 0, \quad i = 1, \ldots, N_{\mathrm{Comp}},$$
$$j = 1, \ldots, N_{\mathrm{Col}} \tag{4}$$

Neglecting the dispersion effects, the inlet concentration of a column is equal to the outlet concentration of the previous column in the series, except for the points of introduction of feed and fresh eluent. Thus, the boundary conditions can be written as:

$$C_i^j(z=0, t) = C_i^{j-1}(z=L, t), \quad i = 1, \ldots, N_{\mathrm{Comp}},$$
$$j = 1, \ldots, N_{\mathrm{Col}} \tag{5}$$

The condition for the nodes between zone IV and zone I takes into account the dilution of the components in the outgoing stream of zone IV before re-entering zone I:

$$C_{I,\,i}^1(z=0, t) = \frac{C_{\mathrm{IV},\,i}^{N_{\mathrm{Col}}}(z=L, t)\dot{V}_{\mathrm{IV}}}{\dot{V}_{\mathrm{IV}} + \dot{V}_{\mathrm{Eluent}}},$$
$$i = 1, \ldots, N_{\mathrm{Comp}} \tag{6}$$

In this equation $\dot{V}_{\mathrm{IV}}$ and $\dot{V}_{\mathrm{Eluent}}$ are the flow-rates of the liquid stream in zone IV and of the eluent make-up, respectively. Between zone II and III the feed is pumped into the system. The concentration at the inlet of zone III thus depends on the concentrations and the flow-rates of the feed stream and the outgoing stream of zone II. Consequently, it holds:

$$C_{\mathrm{III},\,i}(x=0, t) = \frac{C_{\mathrm{II},\,i}(z=L, t)\dot{V}_{\mathrm{II}} + C_{\mathrm{Feed},\,i}\dot{V}_{\mathrm{Feed}}}{\dot{V}_{\mathrm{II}} + \dot{V}_{\mathrm{Feed}}},$$
$$i = 1, \ldots, N_{\mathrm{Comp}} \tag{7}$$

Due to the non-linear character of the isotherm equations, the solution of Eq. (1) requires the use of numerical methods. The fast and stable finite difference algorithm as implemented in the software SMB-Guide (Knauer, Berlin) was used for all calculations. Further details concerning the numerical solution are reported elsewhere [14,15].

3.2. Region of complete separation based on equilibrium theory

A powerful tool to analyze the migration of concentration fronts in a fixed-bed is the classical equilibrium theory [18,19]. The basic equations of this theory are Eq. (1) and Eq. (2) assuming all D_{ap} to be zero. These equations have to be fulfilled for periodically changing boundary conditions in the multi-column arrangement. Recently, several substantial contributions to analyze the SMB process exploiting the analogy to the more simple true moving bed process have been presented [20–22]. The most interesting result for design purposes is the derivation of analytical expressions for the linear velocities, u_j, or the corresponding volumetric flow-rates, $\dot{V}_j$, required in the four zones ($j = \mathrm{I} \ldots \mathrm{IV}$) to achieve the complete separation of a binary feed into two streams containing the pure components. The region of flow-rates fulfilling this condition can be specified as a function of four net flow ratios, m_j, related to the volumetric flow-rates of the liquid and the solid. The latter flow-rate depends for the SMB process on the shifting time t_{shift}. For the net flow ratios holds [20]:

$$m_j = \frac{\dot{V}_j}{\dot{V}_S(t_{\mathrm{shift}})} - \frac{\varepsilon}{1-\varepsilon} \quad j = \mathrm{I} \ldots \mathrm{IV} \tag{8}$$

Most critical for a successful separation are the net flow ratios for the regions II and III upstream and downstream of the feed position, i.e. m_{II} and m_{III}. In

[22] explicit equations are given to calculate regions in the m_{II}, m_{III} plane for the constant selectivity Langmuir model and modified variable selectivity Langmuir models. Performing a superposition of two regions calculated with the Langmuir model approximate equations were derived for a Bi-Langmuir model [15,23]. The size and the shape of the regions of complete separation depend on the isotherm model and the feed concentration. The more concentrated the feed is the smaller the region of available operating parameters becomes. Usually the region has a triangular shape in the m_{II}, m_{III} plane. The equilibrium theory further offers limits for the two other net flow ratios, m_I and m_{IV}, [20–23].

3.3. Perturbation method for adsorption isotherm determination

The knowledge of the adsorption isotherms, Eq. (2), is the main prerequisite for applying the presented mathematical model to simulate the SMB process. Several methods are available for the determination of the equilibrium data [24]. In this study a perturbation method was applied that allows the determination of the parameters of an isotherm model from retention time measurements with mixtures. Thus, no pure components are required for the experiments.

The principle of the perturbation method is based on a stepwise saturation of the column with different known feed concentrations. After reaching equilibrium small samples possessing a different concentration are injected and the corresponding retention times are measured. Fig. 2 illustrates the principle of the perturbation method for a single component dissolved in a non-adsorbable eluent. At zero time a small (analytical) sample size is injected on the not preloaded column. In the following steps the column is saturated at different concentrations and small amounts of pure eluent are injected at the times marked with arrows. Possible deviations of the retention times at higher concentrations are caused by the non-linearity of the adsorption isotherm. Since the method depends only on the analysis of times no detector calibration is necessary.

To determine the competitive isotherms for a binary mixture the same procedure can to be applied saturating the column with different solutions of known concentration of the two components. At each plateau a perturbation induces two pulses. If the isotherms are known, the two corresponding retention times could be predicted analytically. Using the column mass balance equation and the coherence condition introduced in the frame of equilibrium theory [18] the following equations can be derived:

$$t_{R_{i,k}}(\bar{C}) = t_0 \left(1 + \frac{1-\varepsilon}{\varepsilon} \left.\frac{\mathrm{d}q_i}{\mathrm{d}c_i}\right|_{\bar{c}}\right) \quad \text{with}$$

$$\bar{c} = (C_1, C_2) \quad i = 1 \ldots 2, \quad k = 1 \ldots 2 \tag{9}$$

In Eq. (9) t_0 is the retention time of a non-retained component The indices i and k stand for the com-

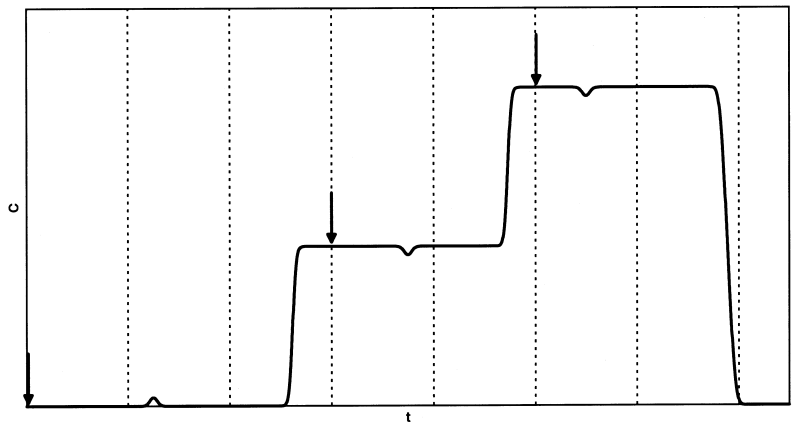

Fig. 2. Principle of the applied perturbation method, illustrated for stepwise increased concentration plateaux of a single component. The arrows mark the time for injecting small samples to perturb an equilibrium state.

ponents and the corresponding retention times. Eq. (9) accounts for the fact that a perturbation introduced at the bed inlet causes traveling waves that reach after well defined retention times the column outlet. According to Eq. (9) 2*2 retention times might exist. However, due to the coherence condition, there are only two distinguishable retention times:

$$t_{R_{1,1}} = t_{R_{2,1}} = t_{R_1}$$
$$t_{R_{1,2}} = t_{R_{2,2}} = t_{R_2} \quad (10)$$

As indicated in Eq. (9), the retention times depend essentially on the total derivatives of the adsorption isotherms. For them holds:

$$\left.\frac{dq_i}{dC_i}\right|_{\bar{c}} = \sum_{j=1}^{N} \left.\frac{\partial q_i}{\partial C_j}\right|_{\bar{c}} \left.\frac{dC_j}{dC_i}\right|_{\bar{c}}, \quad k = 1 \ldots 2 \quad (11)$$

Assuming the validity of an isotherm model, the partial derivatives $\partial q_i/\partial C_j$ can be specified. To determine the required differentials dC_1/dC_2 the following quadratic equation results from the coherence condition delivering two values and thus according to Eq. (9) two different retention times:

$$(dC_1/dC_2|_{\bar{c}})^2 + dC_1/dC_2|_{\bar{c}} \frac{\partial q_2/\partial C_2|_{\bar{c}} - \partial q_1/\partial C_1|_{\bar{c}}}{\partial q_2/\partial C_1|_{\bar{c}}} - \frac{\partial q_1/\partial C_2|_{\bar{c}}}{\partial q_2/\partial C_1|_{\bar{c}}} = 0 \quad (12)$$

The principle of the perturbation method is just the solution of the inverse problem, i.e. the determination of parameters of an isotherm model from measured retention times.

To model the adsorption equilibrium a suitable isotherm equation has to be chosen. For mixtures the model equations are usually coupled to take into account the competition for available adsorption sites. The following modified competitive Langmuir equation was found to represent several sets of experimental data satisfactorily [24,25]:

$$q_i = \frac{a_i C_i}{1 + \sum_{j=1}^{N_{Comp}} b_j C_j} + \lambda_i C_i, \quad i = 1, \ldots, N_{Comp} \quad (13)$$

This equation considers non-competitive and competitive adsorption at different types of adsorption sites and is especially suitable for the description of isotherms of enantiomers on chiral stationary phases.

4. Experimental

4.1. Materials

The separation problem under investigation was the enantioseparation of 1-phenoxy-2-propanol purchased from Fluka (Buchs, Switzerland) and used without further purification. As recommended in the literature [26] the following chromatographic system was applied for the separation:

As stationary phase Chiralcel OD (Daicel Chemical Industries, Tokyo, Japan) with a particle size of 20 μm was used. The mobile phase was *n*-hexane–isopropanol (90:10), provided by Merck (Darmstadt, Germany).

The (−)-enantiomer is the less retained component, with $k'_{(-)} = 1.72$. The (+)-enantiomer is the more retained component, with $k'_{(+)} = 4.58$. The relative large value of the separation factor, $\alpha = 2.66$, indicates that the separation is simple under analytical conditions.

4.2. SMB chromatography

For the experimental investigations a laboratory-scale SMB unit similar to that described by Negawa [3] was used. The system consists of twelve columns (10 cm×1.6 cm I.D., three columns per section) connected to four electric actuated 12-port rotary valves (Valco, Houston, TX, USA). One valve is coupled to the feed pump (Jasco PU-980, Tokyo, Japan), one to the eluent pump (Jasco PU-986), one to the raffinate pump (Jasco PU-980) and the last one to the extract port. The position of the recycle pump (Jasco PU-987) is fixed. The fully automated process is controlled by a computer using laboratory-developed software. To check the stability of the extract stream the volumetric flow-rate was measured with a flow meter (Phase Separations, Deeside, UK). All columns were kept at 22°C in a thermostated water bath.

The packing procedure and the individual characteristics of the columns used were previously described in a study of the SMB separation of a chiral

epoxide [6]. For all columns a high reproducibility of the retention times (standard deviation $<2\%$) of the epoxide enantiomers have been observed.

4.3. Analytical chromatography

To control the composition of the effluents a HP1100 liquid chromatograph equipped with a diode-array detector (Hewlett-Packard, Waldbronn, Germany) was used. The enantiomeric excess in the extract and raffinate and the concentrations of the enantiomers between the columns in the cyclic steady state were determined at a temperature of 22°C on a Daicel Chiralcel OD column (25 cm×0.4 cm I.D.) using *n*-hexane–isopropanol (90:10) as mobile phase and a flow-rate of 1 ml/min. UV-detection was carried out at 220 nm for low concentrated samples and at 285 nm for higher concentrated (>2 g/l) solutions.

4.4. Perturbation measurements

In order to determine the adsorption isotherms of the enantiomers with the described perturbation method a simple chromatographic set-up was applied. The system consists of a HPLC pump (Knauer Mini-Star K-500, Berlin, Germany), a continuous refractive index (RI) detector (Knauer K-2300) and a six-port sample injection valve (Rheodyne 7125, Cotati, CA, USA) equipped with a 100 μl sample loop. The measurements were performed at a temperature of 22°C using one of the columns (10 cm×1.6 cm I.D.) of the SMB separator. The flow-rate in all experiments was 4 ml/min.

5. Determination of adsorption isotherms

In the first stage of the experimental investigations the basic chromatographic data of one of the SMB columns have been determined. The total column porosity was measured by injecting a small sample of hexane, which is considered to be non-retained on the stationary phase. The total void volume was found to be 13.73 ml, leading to a total porosity of $\varepsilon=0.68$. The column efficiency, i.e. the number of theoretical plates, extracted from the peaks obtained for small amounts of racemate injected at a flow-rate of 4 ml/min exceeded 2000 for both enantiomers. This value indicates that the column has been properly packed.

The applied perturbation method is based on successive step changes of the concentration at the column inlet. In the first step the column was equilibrated with pure mobile phase. For the next steps, solutions containing known concentrations of the racemate were pumped through the column. After reaching equilibrium indicated by constant plateau concentrations, a small perturbation (100 μl) was introduced into the system using the injection valve. In case of the non-preloaded column, a diluted sample of the racemate, $C_{(-)}=C_{(+)}=0.1$ g/l, was injected, otherwise pure mobile phase. The retention times of the two induced responses, were recorded using the RI detector. Table 1 summarises the concentrations for all equilibrium states and the obtained retention times. The corresponding chromatograms are superimposed for illustrations in Fig. 3. In order to maintain sensitivity the reference cell of the detector was filled with the equilibrium solution prior the each perturbation. For that reason the concentration steps illustrated in the schematic representation of the perturbation method (Fig. 2) are not visible in Fig. 3. The largest analytical retention times of both enantiomers are given by the peaks

Table 1
Experimental results of the perturbation method for a series of racemic mixtures of increasing concentrations. Column, 10 cm×1.6 cm I.D., packed with 20 μm Chiralcel OD; mobile phase, hexane–isopropanoI (90:10); flow-rate, 4 ml/min

Step	Plateau $C_{(-)}=C_{(+)}$ (g/l)	Retention times	
		$t_{R,1}$ (min)	$t_{R,2}$ (min)
1	0.00	9.31	19.15
2	0.50	9.02	18.46
3	1.01	8.58	16.24
4	1.51	8.12	14.33
5	2.00	7.72	12.90
6	2.50	7.37	11.75
7	3.00	7.05	10.87
8	3.51	6.78	10.28
9	4.01	6.58	9.77
10	4.51	6.40	9.37
11	5.00	6.26	9.04
12	7.51	5.77	7.95
13	10.01	5.44	7.29
14	15.00	5.08	6.12

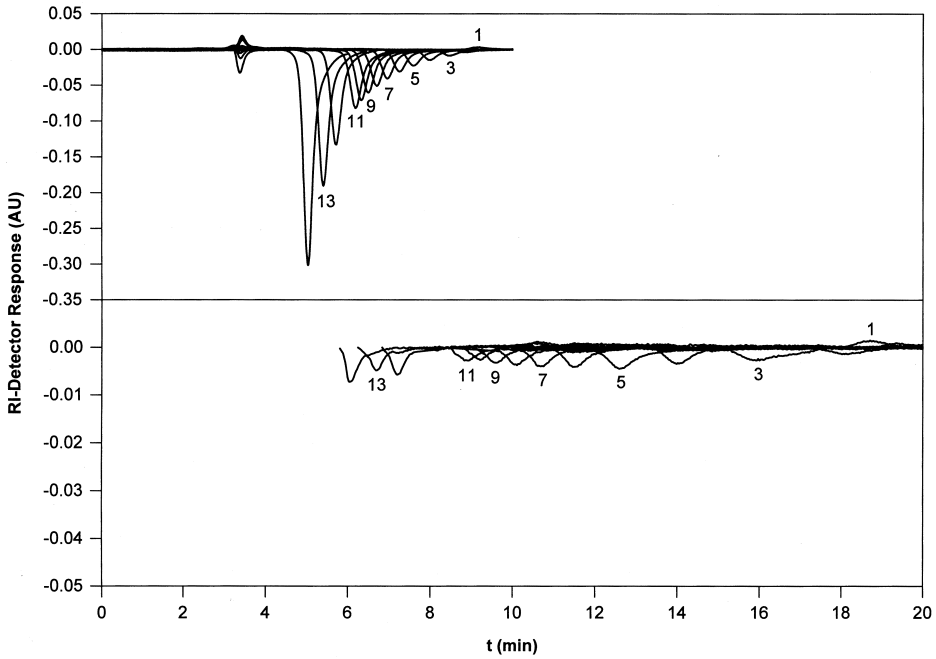

Fig. 3. Experimental responses to small perturbations injected after equilibrating the column at different concentrations. For each equilibrium plateau (1 to 14) the smaller retention time is illustrated on top and the larger retention time is illustrated on the bottom. The experimental conditions are summarised in Table 1.

corresponding to the first step. The shift of the retention times at higher concentrations are caused by the non-linearity of the adsorption isotherms. Fig. 3 also demonstrates that the excellent separation obtainable under analytical conditions is diminishing in case of overloading the column.

The primary data given in Table 1 were converted using Eq. (9) into two total derivatives, dq/dC, for each plateau. By fitting these differentials to the theoretical values based on the isotherm equation Eq. (13) the free parameters were determined. Fig. 4 shows as symbols the total derivatives obtained from the retention times measured. The corresponding best fit theoretical results for the assumed isotherm model are also shown in Fig. 4. The parameters given in Table 2 were obtained by non-linear regression using Marquardt's method [27] minimizing an overall objective function including all data available. There is a relative good agreement between theoretical and experimental data as confirmed also by the low standard deviation for all total isotherm derivatives (Table 2). The obtained agreement was found to be much better then the results achieved in a parallel study with the standard competitive Langmuir equation ($\lambda_i = 0$, in Eq. (13)).

The theoretical isotherms of the single solutes calculated with the determined parameters of Eq. (13) are illustrated in Fig. 5. A major difference between these isotherms is noticeable. The isotherm of the better adsorbable (+)-enantiomer is much more non-linear compared to the isotherm of the less adsorbed (−)-enantiomer.

6. Results and discussion

6.1. Specification of operating conditions for the SMB process

To specify appropriate operating conditions for the separation of the racemic mixture, i.e. to determine suitable net flow ratios m_j within the four SMB zones, at first the region of complete separation in the (m_{II}, m_{III}) plane was calculated using equilibrium theory and the determined isotherm parameters summarised in Table 2 [20–23]. Due to the strong

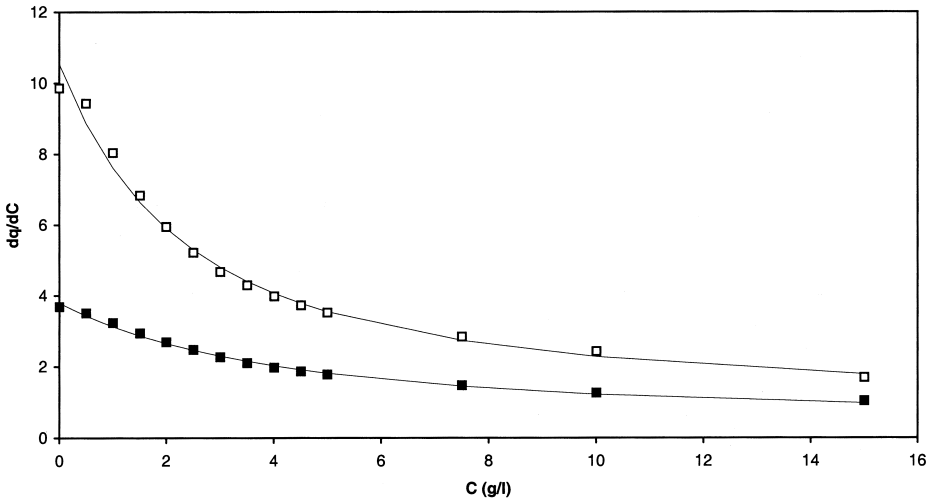

Fig. 4. Total local derivatives of the isotherms belonging to different equilibrium states. Experimental data (■ and □) and theoretical results (solid line) using the modified competitive Langmuir isotherm equation (Eq. (13)).

non-linearity of the isotherms, the region was found to be small for higher feed concentrations. Therefore, for further experimental studies the feed concentration was limited to $C_{(-)}=C_{(+)}=12.5$ g/l. The corresponding region of complete separation for these concentrations is shown in Fig. 6. In the figure are also illustrated four operating points chosen for the experimental runs. The consideration of the relative position of the operating point in the m_{II}, m_{III} plane with respect to the region of complete separation allows to estimate the purities of the two outlets [22]. Operating the SMB unit under conditions corresponding to the two points inside the triangular region (1 and 2) a complete separation of the racemic mixture can be expected. In contrast, an operation related to point 3 should lead to a pure extract but the purity of the raffinate is supposed to drop below 100%. The opposite situation is expected for point 4. Compared to point 1 a higher productivity is expected in operating point 2, since this point is closer to the vertex of the region which represents maximum productivity [22]. However, operating points located close to the border of the region of complete separation are less robust. That means small fluctuations of the process parameters might cause insufficient performance. Due to this fact and due to the underlying model assumptions (neglecting all kinetic effects, assuming a true moving bed) operating points targeting a complete separation should be kept away from the region borders. The chosen operating conditions, i.e. the feed concentration, the external and internal flow-rates, the switching time and the net flow ratios, corresponding to the four designated operating points are given in

Table 2
Model parameters used in calculations

Columns and system		Isotherm equation	(−)-enantiomer	(+)-enantiomer
Number of columns	12	a (l/l)	3.28	9.81
Columns in zone I/II/III/IV	3/3/3/3	b (l/g)	0.031	0.183
L (cm)	10	λ (l/l)	0.512	0.749
d (cm)	1.6	σ (%)	2.6	
ε	0.68			
N_P per column	150			

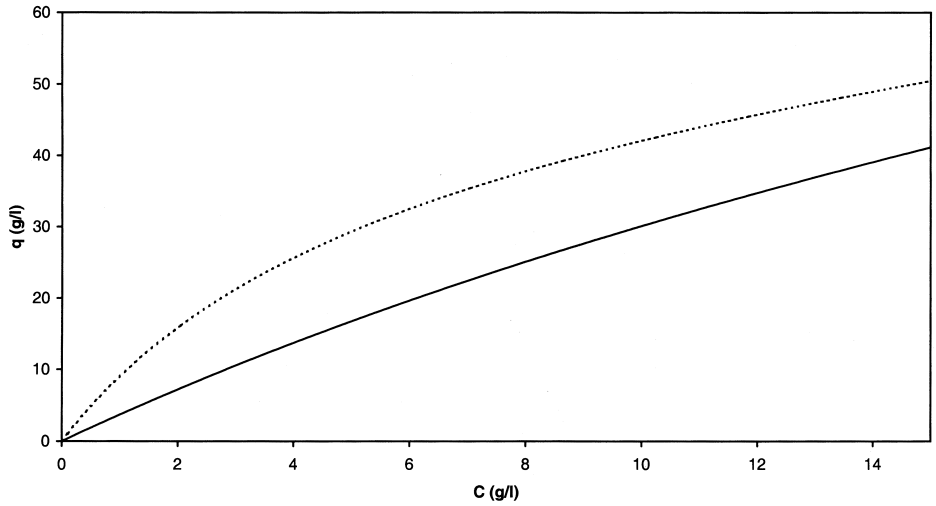

Fig. 5. Theoretical single solute isotherms of the (−)-enantiomer (solid) and the (+)-enantiomer (dotted) calculated with the modified Langmuir equation (Eq. (13)) and the parameters in Table 2.

Table 3. The net flow ratios for zones I and IV were specified based on the limits considerations offered by equilibrium theory and on the results of a priori simulations using the equilibrium-dispersion model. For the latter calculations as a conservative estimation 150 theoretical plates per column were assumed per column to calculate the apparent dispersion coefficient according to Eq. (3).

6.2. Experimental verification

To demonstrate the usefulness of the described procedure for the specification of appropriate operating conditions and to verify the proposed mathematical model, experimental results were compared with numerical predictions. Four SMB runs were performed using the operating parameters presented

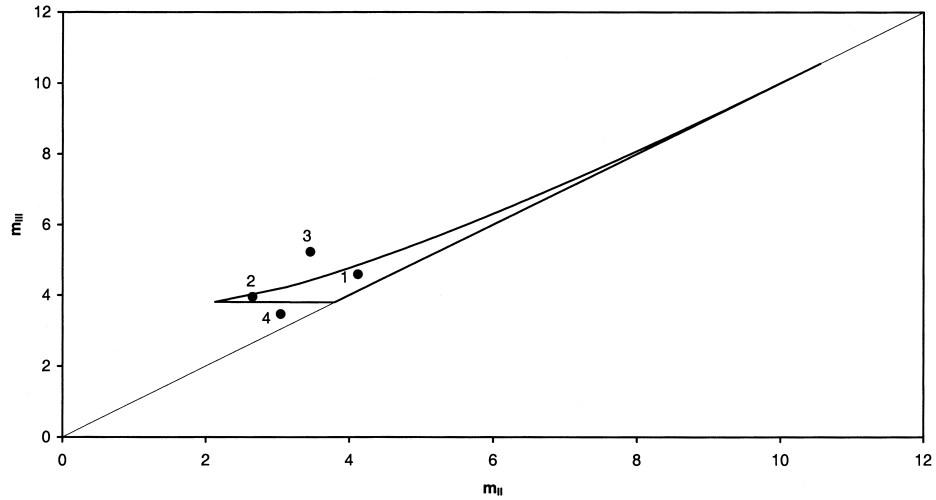

Fig. 6. Separation of the racemate in the lab-scale SMB unit. Region of complete separation (solid line) in the (m_{II}, m_{III}) plane for a feed concentration of $C_{(-)}=C_{(+)}=12.5$ g/l calculated with the parameters given in Table 2. The four operating points (●) correspond to the experimental SMB runs and the conditions summarised in Table 3.

Table 3
Conditions of the four investigated operating points used for the SMB separation of the racemate

Parameter	Operating point			
	1	2	3	4
$C_{Feed,(-)} = C_{Feed,(+)}$ (g/l)	12.5			
t_{Shift} (min)	10	9	12	10
$\dot{V}_{Feed}$ (ml/min)	0.300	0.921	0.935	0.268
$\dot{V}_{Eluent}$ (ml/min)	7.000	6.022	5.844	5.418
$\dot{V}_{Extract}$ (ml/min)	5.000	5.951	4.574	5.112
$\dot{V}_{Raffinate}$ (ml/min)	2.300	0.992	2.205	0.574
$\dot{V}_{I}$ (ml/min)	9.000	9.356	7.547	8.417
$\dot{V}_{II}$ (ml/min)	4.000	3.405	2.973	3.305
$\dot{V}_{III}$ (ml/min)	4.300	4.326	3.908	3.573
$\dot{V}_{IV}$ (ml/min)	2.000	3.334	1.703	2.999
m_{I}	11.964	11.055	12.122	11.113
m_{II}	4.121	2.653	3.458	3.043
m_{III}	4.591	3.953	5.229	3.466
m_{IV}	0.983	2.553	1.052	2.560

in Table 3. The extract and raffinate was collected and analysed for each cycle defined by the time interval between two consecutive column shifts, t_{shift}. After reaching the cyclic steady-state, the process was stopped in the middle of the switching period and the concentration profiles within the system were determined by measuring the concentrations at each column outlet. The corresponding numerical predictions of the dynamic behaviour of the SMB were calculated based on the model parameters given in Table 2. The calculated concentrations at the draw-off nodes were averaged for each cycle. The purities and recovery yields achieved and the concentrations of both isomers at the draw-off nodes obtained under steady-state conditions are summarised in Table 4, both for the experiments and for the predictions.

Fig. 7 illustrates the internal concentration profiles of both enantiomers along the columns of the SMB obtained for operating point 1 after reaching the cyclic steady-state. The predicted profiles are shown just after and before a switching operation. The experimental data were measured at $t_{shift}/2$. Although the values show some scatter, the general shape of the experimental profiles is well represented by the model predictions. For both enantiomers most experimental points are located between the two calculated limit profiles. It should be noted that the oscillations seen on the plateaux of the predicted profiles of the (+)-enantiomer result from the periodic nature of the SMB, and are not caused by a numerical instability in the calculation of the equilibrium-dispersive model [28]. The corresponding experimental and predicted averaged concentration histories at the product ports are presented in Fig. 8. The extract concentrations are shown at the top, the raffinate concentrations at the bottom of the figure. As estimated by constructing the separation region in the m_{II}, m_{III} plane a complete separation is observed for the designated operating conditions. The extract stream contains purely the more retained (+)-enantiomer, while the raffinate stream carries only the less retained (−)-enantiomer. Furthermore, the predicted concentrations of extract and raffinate in the cyclic steady-state are in good agreement with the measured data. The dynamic behaviour of the SMB is also well described by the equilibrium-dispersive model. Similar to the theoretical results, the periodic steady-state is reached in the experiments after four

Table 4
Experimental (exp.) and predicted (sim.) performance parameters for the four SMB runs investigated

Parameter	Operating point							
	1		2		3		4	
	exp.	sim.	exp.	sim.	exp.	sim.	exp.	sim.
$Pu_{Extract}$ (%)	100	100	97.0	100	100	100	89.8	79.5
$Pu_{Raffinate}$ (%)	100	100	100	100	74.4	68.4	100	99.7
$REC_{(+)}$ (%)	100	100	100	100	65.4	54.2	99.8	100
$REC_{(-)}$ (%)	100	100	96.8	100	100	100	73.6	89.1
$C_{Extract,(+)}$ (g/l)	0.79	0.73	1.93	1.87	1.65	1.39	0.64	0.64
$C_{Extract,(-)}$ (g/l)	0.00	0.00	0.06	0.00	0.00	0.00	0.16	0.07
$C_{Raffinate,(+)}$ (g/l)	0.00	0.00	0.00	0.00	1.82	2.44	0.01	0.00
$C_{Raffinate,(-)}$ (g/l)	1.77	1.85	10.68	11.76	5.29	5.46	4.07	5.26

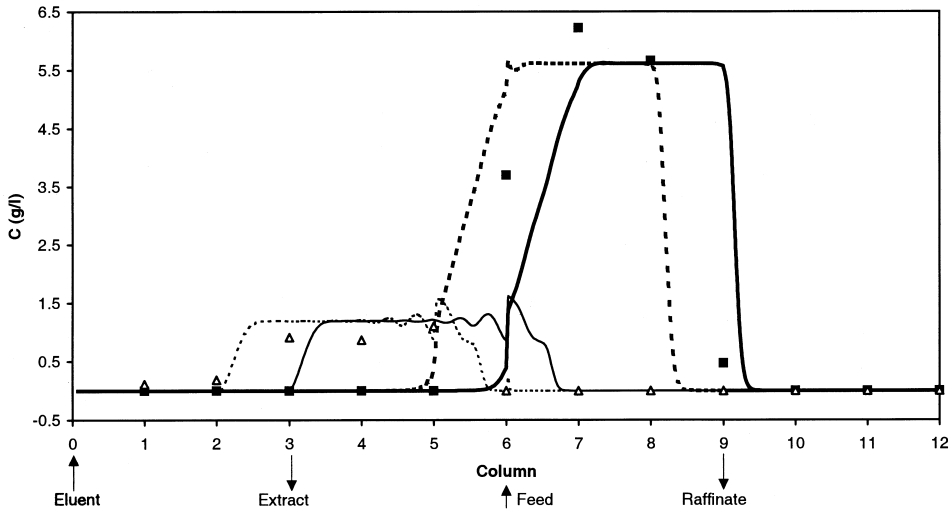

Fig. 7. Experimental and predicted internal concentration profiles for the separation of the racemate using operating point 1 in Table 3. Experimental data ((−)-enantiomer: ■, (+)-enantiomer: △) were taken at half time period in the cyclic steady state. Theoretical data ((−)-enantiomer: thick lines, (+)-enantiomer: thin lines) illustrate the band profiles along the columns just after switching (dotted) and just before switching (solid). Calculations are based on the parameters given in Table 2.

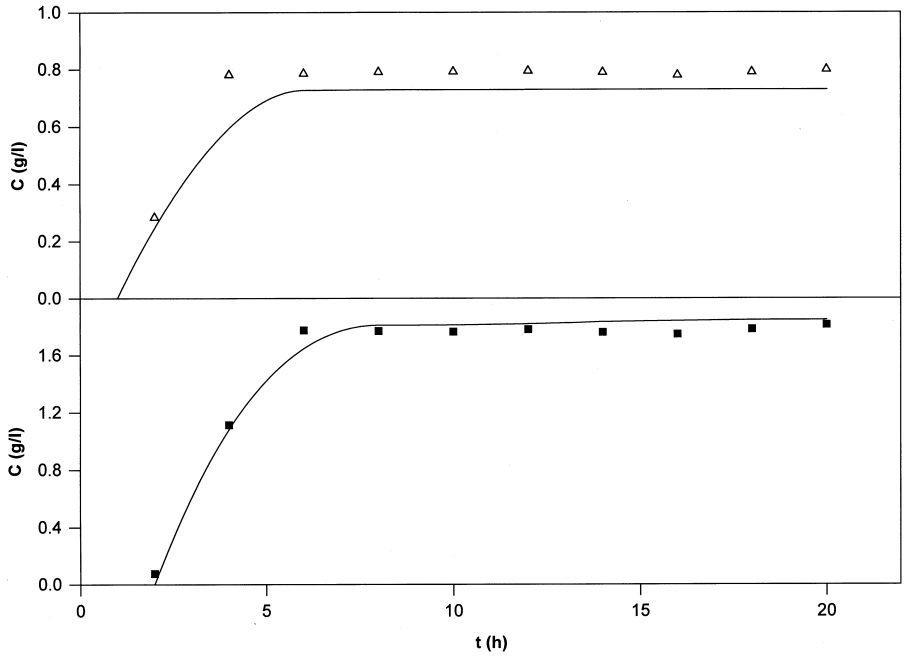

Fig. 8. Experimental and predicted history of concentrations at the extract (top) and the raffinate (bottom) outlet of the SMB unit. Separation of the racemate using operating point 1 in Table 3. The experimental [(−)-enantiomer: ■, (+)-enantiomer: △] and theoretical data (solid lines) are averaged over one cycle. Calculations are based on the parameters given in Table 2.

cycles. Due to the fact that the agreement between experimental and calculated data is better for the concentration histories at the product ports than for the internal profiles, it might be supposed that the discrepancies in Fig. 7 are mainly caused by inaccuracies of the concentration measurements.

A presentation similar to Figs. 7 and 8 is given in Figs. 9 and 10 for operating point 2 respectively. In general, the agreement of measured and calculated data is of the same quality as for operating point 1. However, the measured steady-state profiles along the columns exhibit a noticeable tailing in the direction of the solid stream which is not well accounted for by the model. Therefore, the resolution observed is, in reality, somewhat less than the calculated one. It can be recognised from Fig. 10 that the extract stream contains small amounts of the (−)-enantiomer. Thus, the purity of the extract drops to 97% in the experiment, while the model predicts a purity of 100%. This inaccuracy confirms the suggestion mentioned above, that operating points located close to the boundaries of the complete separation region in the m_{II}, m_{III} plane should be avoided, when purities of 100% for both product streams are required. It should be noted that in this run, due to the displacement effect averaged concentrations of the (−)-enantiomer above the feed concentration, were recorded (Fig. 9).

Finally, Figs. 11 and 12 show the concentration histories at the product ports for the two operating points 3 and 4 located outside the region of complete separation in Fig. 6. As suggested in the previous section the operation of the SMB under these conditions leads either to an impure raffinate (point 3, Fig. 11) or to an impure extract (point 4, Fig. 12). Consequently the corresponding recovery yields drop below 100%. Although the agreement between measured and predicted values is not quantitative, it is evident that the theoretical curves calculated with the equilibrium-dispersive model and the proposed numerical algorithm provide a good representation of the experimental data and reflect the described tendencies.

6.3. Comparison of different isotherm determination methods

The presented results confirm the general reliability of the proposed mathematical model and the applicability of the perturbation method used for the quantification of the required competitive adsorption isotherms. To evaluate the accuracy of the latter, the isotherms of both enantiomers were determined additionally with the classical static adsorption–desorption method [24]. The obtained parameters of Eq. (13) are given in Table 5. In order to quantify

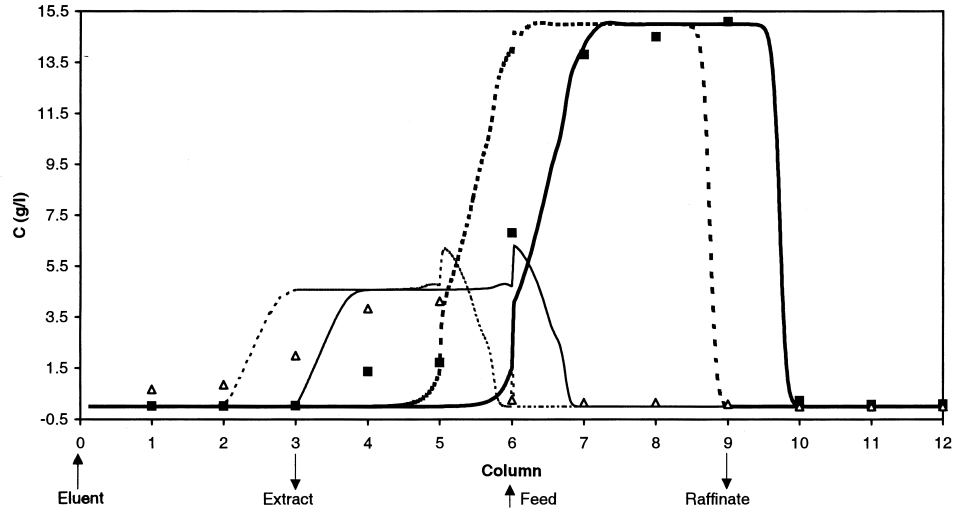

Fig. 9. Experimental and predicted internal concentration profiles for the separation of the racemate using operating point 2 in Table 3. Same conventions as for Fig. 7.

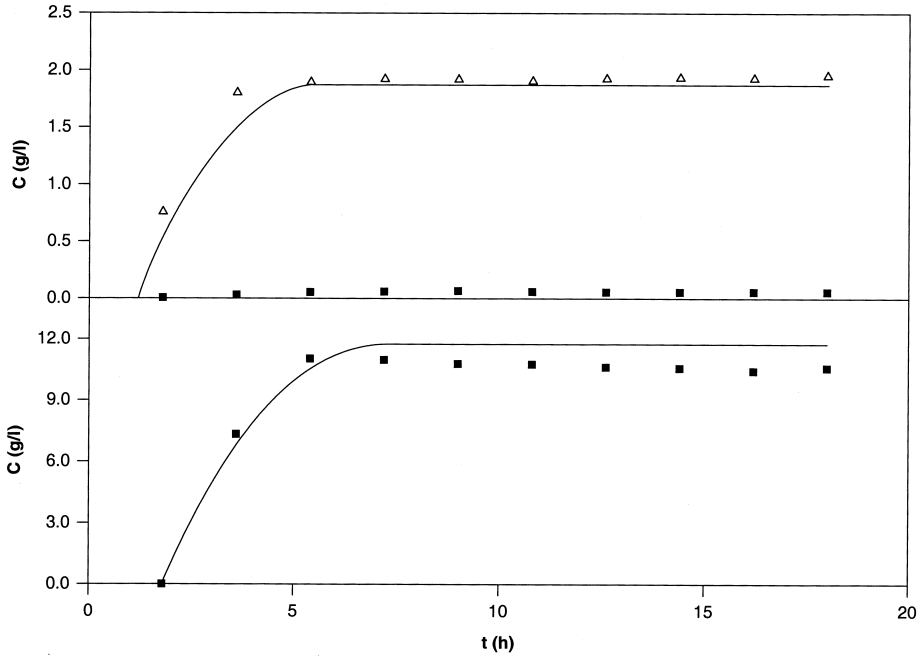

Fig. 10. Experimental and predicted history of concentrations at the extract (top) and the raffinate (bottom) outlet of the SMB unit. Separation of the racemate using operating point 2 in Table 3. Same conventions as for Fig. 8.

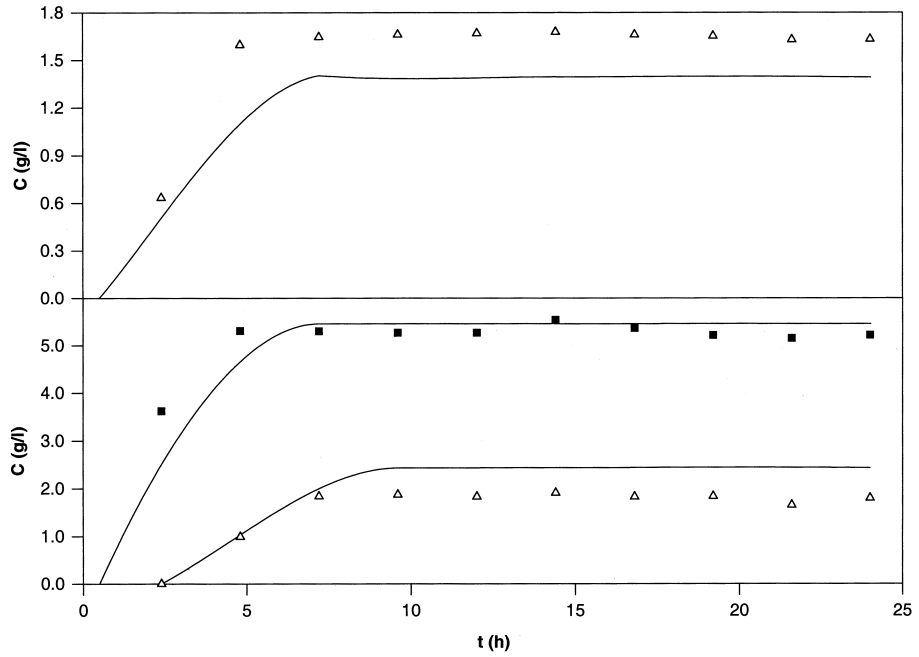

Fig. 11. Experimental and predicted history of concentrations at the extract (top) and the raffinate (bottom) outlet of the SMB unit. Separation of the racemate using operating point 3 in Table 3. Same conventions as for Fig. 8.

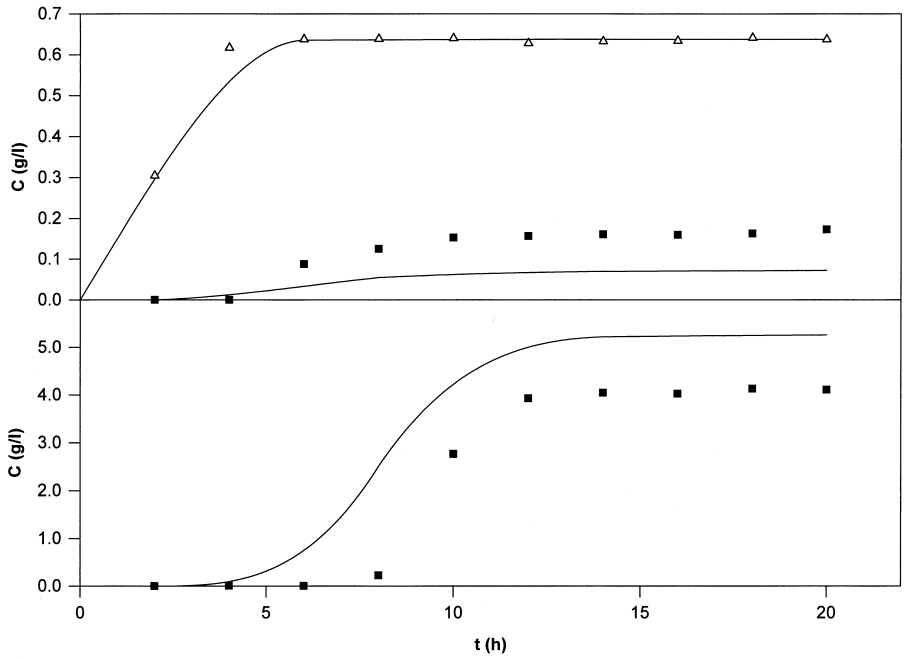

Fig. 12. Experimental and predicted history of concentrations at the extract (top) and the raffinate (bottom) outlet of the SMB unit. Separation of the racemate using operating point 4 in Table 3. Same conventions as for Fig. 8.

the influence of the different isotherm parameters (Tables 2 and 5) on the resulting region of complete separation, calculations were performed for a feed concentration of $C_{(-)}=C_{(+)}=3.125$ g/l using both parameter sets. The two obtained separation regions are superimposed in the m_{II}, m_{III} plane in Fig. 13. The illustration demonstrates that operating points close to the borders of the region are uncertain due to possible inaccuracies of the determined adsorption isotherms. Although there is considerable difference between the corresponding isotherm parameters, the effect on the separation region is less pronounced. The intersection area of both regions is only about 10% smaller than an overall region. That result is considered as a confirmation for the applicability of both methods to determine the adsorption isotherms for designing the SMB process.

Table 5
Adsorption isotherm parameters determined from adsorption–desorption measurements

Isotherm equation	(−)-enantiomer	(+)-enantiomer
a (l/l)	4.02	11.52
b (l/g)	0.064	0.184
λ (l/l)	0.463	0
σ (%)	5.1	

Finally, with the isotherm parameters determined using the adsorption–desorption method (Table 5) the predictions of the internal concentration profiles along the columns were compared with experimental data. Fig. 14 shows the results obtained for the conditions corresponding to operating point 2. Compared to Fig. 9, where the calculation of the profiles is based on the isotherm parameters from perturbation measurements (Table 2), the data predicted with the isotherms from adsorption–desorption measurements describe the experimental profiles a bit more accurate. Mainly, the observed tailing in the direction of the solid stream leading to an impure extract is better accounted for.

7. Conclusions

Modelling of the SMB process can be achieved provided the adsorption isotherms for the relevant components are known. To determine these functions

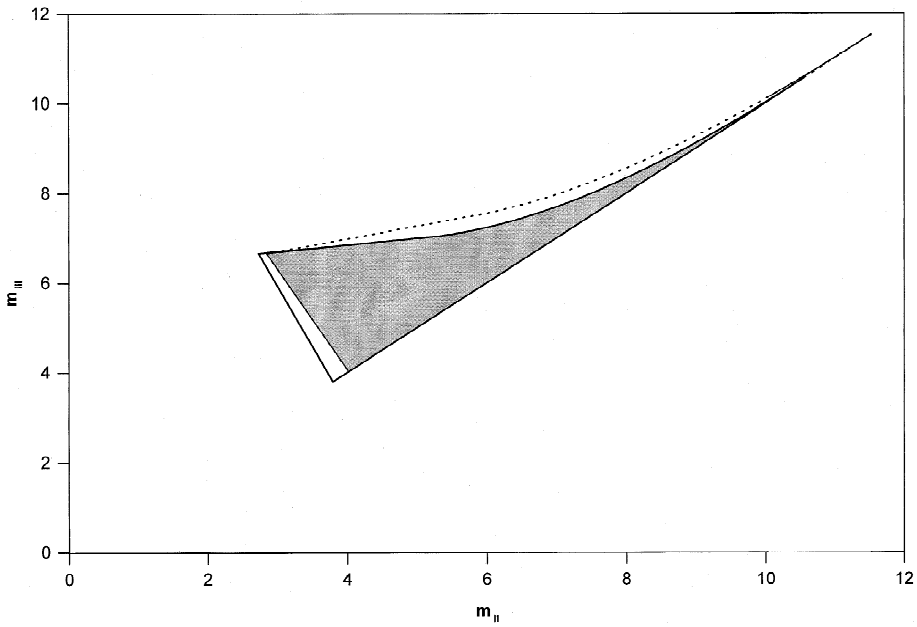

Fig. 13. Comparison of the predictions of the regions of complete separation in the (m_{II}, m_{III}) plane based on different isotherm parameters for a feed concentration of $C_{(-)}=C_{(+)}=3.125$ g/l. The solid line was calculated using the isotherm parameters determined with the perturbation method (Table 2). The dotted line is based on the isotherm parameters determined from adsorption–desorption measurements (Table 5). The shaded area represents the common region.

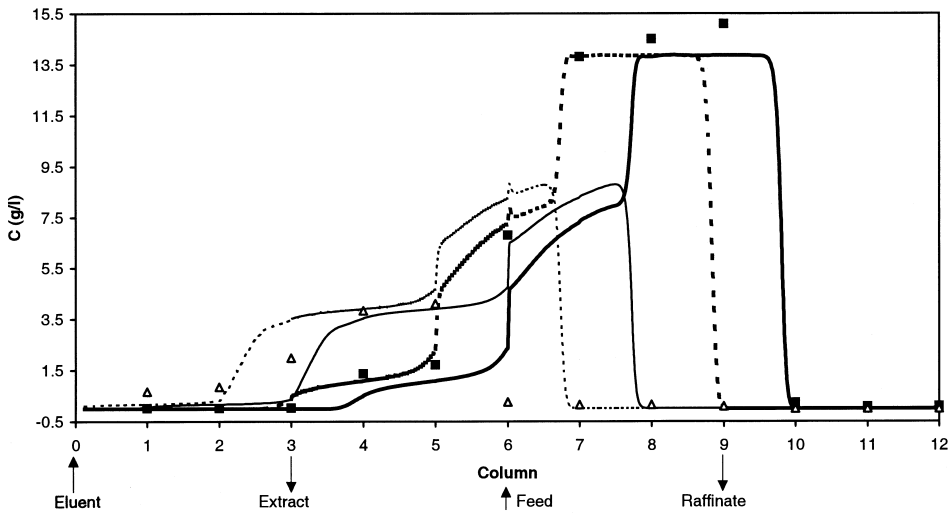

Fig. 14. Experimental and predicted internal concentration profiles for the separation of the racemate using operating point 2 in Table 3. Different to Fig. 9 the theoretical data were calculated using the isotherm parameters in Table 5 determined with the classical adsorption–desorption method. Same conventions as for Fig. 7.

a perturbation method was applied successfully. The presented method allows the determination of competitive adsorption isotherms based on experiments with racemic mixtures.

Internal and effluent concentrations with an equilibrium-dispersive model and based on adsorption isotherms described by a modified competitive Langmuir equation are in good agreement with experimental profiles for different operating conditions. To specify operating conditions to achieve a certain process goal the equilibrium theory delivers reliable estimates. The applied software package SMB-Guide (Knauer, Berlin) was found to be suitable for performing the mentioned calculations in a efficient way on a Personal Computer.

The enantiomers of 1-phenoxy–2-propanol were completely separated on a SMB unit with Chiralcel OD as stationary phase. Robust process parameters were identified that allow for the manufacturing of highly purified (100% e.e.) enantiomers with averaged concentrations of 0.79 g/l [for the (+)-enantiomer] at the extract port and 1.77 g/l [for the (−)-enantiomer] at the raffinate port, respectively.

8. Symbols

a	Parameter in isotherm equation, Eq. (13)
b	Parameter in isotherm equation, Eq. (13)
C	Liquid phase concentration
d	Column diameter
D_{ap}	Apparent dispersion coefficient, Eq. (3)
L	Column length
m	Net flow ratio, Eq. (8)
N_{Col}	Number of columns
N_{Comp}	Number of components
N_p	Number of theoretical plates
Pu	Purity
q	Solid-phase concentration
t	Time
t_0	Retention time of a non-retained component
t_{inj}	Time of injection
t_R	Retention time
t_{shift}	Switching time
u	Linear velocity
V	Volume of the column
$\dot{V}$	Volumetric flow-rate
REC	Recovery yield
z	Axial coordinate of column

Subscripts

(−)	First eluted enantiomer
(+)	Second eluted enantiomer
I . . . IV	zone of the SMB
Eluent	EIuent stream
Extract	Extract stream
Feed	Feed stream
i	Component
j	Column
n	SMB zone index
Raffinate	Raffinate stream

Greek

ε	Total porosity
λ	Parameter in isotherm equation, Eq. (13)
σ	standard deviation,

$$\sigma = 100\% \sqrt{\frac{1}{N_D - N_{PA}} \sum_{i=1}^{N_p} \left(\frac{q_{i,ex} - q_{i,th}}{q_{i,ex}} \right)^2}$$

with N_D and N_{PA} being the numbers of data and model parameters, respectively.

References

[1] D.B. Broughton, C.G. Gerhold, US Pat. 2 985 589 (1961).
[2] R.M. Nicoud, LC·GC Int. 5 (1992) 43.
[3] M. Negawa, F. Shoji, J. Chromatogr. 590 (1992) 113.
[4] C.B. Ching, B.G. Lim, E.J.D. Lee, S.C. Ng, J. Chromatogr. 634 (1993) 215.
[5] R.-M. Nicoud, G. Fuchs, P. Adam, M. Bailly, E. Küsters, F.D. Antia, R. Reuille, E. Schmid, Chirality 5 (1993) 267.
[6] E. Küsters, G. Gerber, F.D. Antia, Chromatographia 40 (1995) 387.
[7] F. Charton, R.M. Nicoud, J. Chromatogr. A 702 (1995) 97.
[8] M.J. Gattuso, B. McCulloch, D.W. House, W.M. Baumann, K. Gottschall, Pharm. Tech. Eur. 6 (1996) 20.
[9] D.W. Guest, J. Chromatogr. A 760 (1997) 159.
[10] L.S. Pais, J.M. Loureiro, A.E. Rodrigues, Chem. Eng. Sci. 52 (1997) 245.
[11] E. Cavoy, M.F. Deltent, S. Lehoucq, D. Miggiano, J. Chromatogr. A 769 (1997) 49.
[12] M. Schulte, R. Ditz, R.M. Devant, J.N. Kinkel, F. Charton, J. Chromatogr. A 769 (1997) 93.
[13] E. Francotte, P. Richert, J. Chromatogr. A 769 (1997) 101.

[14] H. Kniep, C. Blümel, A. Seidel-Morgenstern, Fundamentals of Adsorption 6, Ed. F. Meunier, Elsevier, in press.
[15] H. Kniep, Ph.D. Thesis, University of Magdeburg, 1998.
[16] D.M. Ruthven, C.B. Ching, Chem. Eng. Sci. 44 (1989) 1011.
[17] G. Guiochon, S.G. Shirazi, A.M. Katti, Fundamentals of Preparative and Nonlinear Chromatography, Academic Press, San Diego, 1994.
[18] F.G. Helfferich, G. Klein, Multicomponent chromatography, Marcel Dekker, New York, 1970.
[19] H.-K. Rhee, R. Aris, N.R. Amundson, Phil. Trans. Roy. Soc. London A276 (1970) 419.
[20] M. Mazzotti, G. Storti, M. Morbidelli, AIChE J. 40 (1994) 1825.
[21] M. Mazzotti, G. Storti, M. Morbidelli, AIChE J. 42 (1996) 2784.
[22] M. Mazzotti, G. Storti, M. Morbidelli, J. Chromatogr. A 769 (1997) 3.
[23] A. Gentillini, C. Migliorini, M. Mazotti, M. Morbidelli, J. Chromatogr. A 805 (1998) 37.
[24] R.M. Nicoud, A. Seidel-Morgenstern, Isol. Purif. 2 (1996) 165.
[25] R.M. Nicoud, M. Bailly, J.N. Kinkel, R.M. Devant, T.R.E. Hampe, E. Küsters, in: R.M. Nicoud (Ed.), Simulated Moving Bed: Basics and Applications, Institut National Polytechnique de Lorraine, 1993.
[26] T. Shibata, K. Mon, Y. Okamoto, in: A.M. Krstulovic (Ed.), Chiral Separations by HPLC, 1989.
[27] D.W. Marquardt, J. Soc. Appl. Math. 11 (1963) 431.
[28] T. Yun, G. Zhong, G. Guiochon, AIChE J. 43 (1997) 935.